POLİTEKNİK DERGİSİ

JOURNAL of POLYTECHNIC

ISSN: 1302-0900 (PRINT), ISSN: 2147-9429 (ONLINE)
URL: http://dergipark.org.tr/politeknik

Performance comparison of guided mortar projectiles with fixed and moving fins

Sabit ve hareketli kanatlar ile güdümlü havan mermilerinin performans karşılaştırması

***Yazar(lar) (Author(s))**: Bülent ÖZKAN[1], Harun GÖKÇE[2]*

ORCID[1]: 0000-0003-3112-9723

ORCID[2]: 0000-0002-2702-0111

To cite to this article: Özkan B., Gökçe H., "Performance comparison of guided mortar projectiles with fixed and moving fins", ***Journal of Polytechnic***, 27(3): 1101-1108, (2024).

Bu makaleye şu şekilde atıfta bulunabilirsiniz: Özkan B., Gökçe H., "Performance comparison of guided mortar projectiles with fixed and moving fins", ***Politeknik Dergisi***, 27(3): 1101-1108, (2024).

Erişim linki (To link to this article): http://dergipark.org.tr/politeknik/archive

DOI: **10.2339/politeknik.1173585**

Performance Comparison of Guided Mortar Projectiles with Fixed and Moving Fins

Sabit ve Hareketli Kanatlar ile Güdümlü Havan Mermilerinin Performans Karşılaştırması

Highlights

- *The design of a guidance kit which makes the mortar projectiles become guided when released from aerial platforms and the relevant computer simulations performed upon a selected projectile model are investigated.*
- *Different configurations are considered based on the rotational degree of freedom of a pair of fins mounted on a rotary ring.*
- *Final miss distance and time of flight values obtained for all the designated cases are compared.*

Graphical Abstracts

The guidance kit which is mounted upon the nose of the unguided mortar projectile is composed of a fuze, rotor outer ring having a pair of control fins, i.e. fins, actuator rotating the rotor outer ring, sensors, electronic cards, and battery as depicted in this figure.

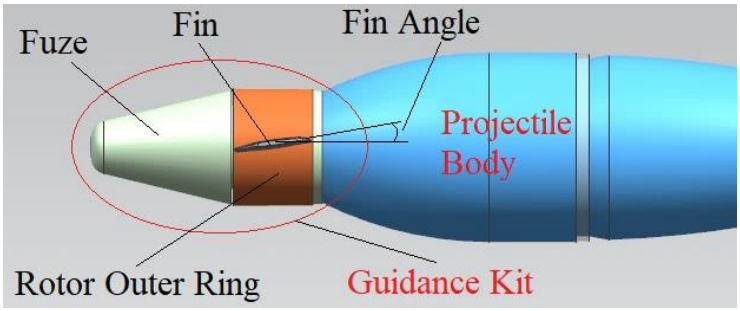

Figure. Considered Guidance Kit Geometry

Aim

This study investigated the effects of the performance comparison of guided mortar projectiles with fixed and moving fins.

Design & Methodology

Analytical calculations are made on the motion equations of the guided mortar projectile.

Originality

The design of a guidance kit which makes the mortar projectiles become guided when released from aerial platforms and the relevant computer simulations performed upon a selected projectile model are investigated.

Findings

It is observed that the rotating find lead smaller miss distance for the shortest autopilot switching duration considered for both windless and windy cases. Once the switching duration increases, the smaller miss distance is attained with the fixed fins.

Conclusion

An interesting point shown from the acquired data is that the final miss distance quantities do not change for the same switching duration when the fin angle becomes different. However, the guided projectile with the fixed fins have a growing pattern as the fin angle gets larger.

Declaration of Ethical Standards

The authors of this article declare that the materials and methods used in this study do not require ethical committee permission and/or legal-special permission.

Performance Comparison of Guided Mortar Projectiles with Fixed and Moving Fins

Araştırma Makalesi / Research Article

Bülent ÖZKAN[1], Harun GÖKÇE[2*]

[1]Faculty of Engineering, Department of Mechanical Engineering, Gazi University, Turkey
[2]Faculty of Technology, Department of Industrial Design Engineering, Gazi University, Turkey

(Geliş/Received : 10.10.2022 ; Kabul/Accepted : 10.03.2023 ; Erken Görünüm/Early View : 02.04.2023)

ABSTRACT

Guidance munition has become one of the popular subjects in both the theoretical and applicable studies since they could find a wide field of use in recent years because of their high performance and lower collateral damage capabilities as per the improving defence concept. The use of smaller and lighter guided munition makes the stated advantages increase without relinquishing the effectiveness. In this study, the design of a guidance kit which makes the mortar projectiles become guided when released from aerial platforms and the relevant computer simulations performed upon a selected projectile model are investigated. Here, two different configurations are considered based on the rotational degree of freedom of a pair of fins mounted on a rotary ring. In the simulations in which it is assumed that the guided projectile is released from an unmanned aerial vehicle, the different values of the fin deflection, autopilot switching duration, and side wind are considered for both of the mentioned geometries. Finally, the final miss distance and time of flight values obtained for all the designated cases are compared.

Keywords: Guided mortar projectile, guided projectile released from aerial platforms, control with fins, controls with rotating fins, guidance and control.

Sabit ve Hareketli Kanatlar ile Güdümlü Havan Mermilerinin Performans Karşılaştırması

ÖZ

Gelişen ve değişen savunma konsepti kapsamında, güdümlü mühimmatlar, yüksek başarım ve düşük tali hasar özellikleri dolayısıyla son yıllarda oldukça popüler bir araştırma alanı haline gelmiş olup bu konuda birçok teorik ve uygulamalı çalışma yapılmıştır. Bilhassa küçük ve hafif güdümlü mühimmat kullanımı, etkinlikten taviz vermeksizin bahsedilen üstünlüklerin elde edilmesini olanaklı kılmaktadır. Bu çalışmada, hava platformlarından atıldığı varsayılan havan mermilerini güdümlü hale getirmek amacıyla kullanılan bir güdüm kitinin tasarımı ele alınmakta ve belirtilen çerçevede gerçekleştirilen bilgisayar benzetimlerinin sonuçları sunulmaktadır. Bu kapsamda, güdüm kiti üzerindeki dönel halkaya bütünlenen bir çift kanatçığın serbestlik derecesine bağlı olarak iki farklı konfigürasyon üzerinde durulmaktadır. Güdümlü havan mermisinin düşük seyir hızlı bir insansız hava aracından bırakılması durumunu göz önüne alan bilgisayar benzetimlerinde, kanatçık açısı, otopilot anahtarlama süresi ve yan rüzgâr parametrelerinin farklı değerleri, bahis konusu konfigürasyonların her ikisi için de uygulanmaktadır. Çalışmanın sonunda, nihai hedeften sapma miktarı ve uçuş süresi değerleri, oluşturulan eşleşme koşullarının tamamı için hesaplanarak karşılaştırılmaktadır.

Anahtar Kelimeler: Güdümlü havan mermisi, hava platformlarından bırakılan güdümlü mermi, kanatçıklı denetim, dönel kanatçıklı denetim, güdüm ve denetim.

1. INTRODUCTION

In accordance with the improvements in the technology, the mass demolition approach has been replaced by the point destruction. This way, it has become possible to attain the cost effectiveness and minimum colateral damage requirements apart from the high performance demand. In this context, guided munitions have been developed by regarding guidance and control algorithms designed as per certain technical specifications [1]. Actually, the guidance and control problem constitutes a wide area for the control of aerial platforms as well as munitions [2, 3, 4].

Depending on whether the design of the explosive part is included in the entire system, the guided munitions can be divided into two main groups. In this sense, missiles constitute the first class since their explosive parts are designed within the whole munition development process. The second group involves the smart bombs built by mounting specifically designed guidance kits upon existing general purpose bombs. Actually, guided projectiles are involved in the latter class because they are the composition of the guidance kits with unguided projectiles [1].

*Sorumlu Yazar (Corresponding Author)
e-posta : harungokce@yahoo.ca

The guided projectiles are usually lighter in mass and smaller in size than the missiles and smart bombs. This provides the users with releasing more munitions towards designated target points. Looking at the available guided projectiles around the world, it is seen that they are intended to be fired from launchers deployed on ground against prescribed stationary surface targets. In those munitions, one of the control strategies below is considered in order to reach the desired guidance and control effectiveness [1, 5]:

- Reaction jet control,
- Control with high frequency piezoelectric actuators,
- Use of internal components,
- Control with reverse rotation,
- Use of nose actuation kits.

In the selection of the most convenient control approach, the first attempt is upon the establishing a convenient mathematical model for the projectile under consideration [6-8]. In this extent, one of the most significant considerations is the endurance of the relevant munition against the high acceleration loads occurring in firing through the launcher [1, 7-10]. Actually, this issue is more critical for the surface-to-surface guided projectiles than the air-to-surface configurations due to the effect of the booster resulting high amount of linear acceleration [11, 12].

In the sense of control of the guided projectiles, several schemes are developed regarding the effectiveness of the application [13-17]. In this extent, certain control approaches including robust algorithms are designed for the elimination of the diverting effects of the disturbances and noise [18, 19]. The roll control of guided mortars comes into the the picture a specific implementation of this problem [20]. Also, several guidance laws are proposed in accordance with the considered engagement problem in the sense of trajectory planning of the guided projectiles [21-24].

Regarding the guided projectiles, the munitions with fixed fins in canard type are also examined in addition to the rotating ones [25]. Among these works, the guidance and control schemes regarding sensor and actuator constraints are also suggested [26]. The fuzzy logic-based integrated guidance and control schemes constitutes another class of the projectile guidance [27].

One of the consequences of the inclusion of the unmanned air vehicles into the defence scheme appears as the need of lighter but effective munitions. In this extent, the guided projectiles seem to be viable candidates for air-to-surface applications. It is obvious that the success of such munitions is related to the performance characteristics of the chosen control approach [1, 10]. The present examples to the air-to-surface guided projectiles can be given as in Figure 1, Figure 2, and Figure 3.

In this study, the engagement capabilities of two guided projectiles composed of a 120 mm mortar projectile and guidance kit mounted on the nose part of the projectile are investigated. Here, the control of the projectile is performed by means of a rotary ring upon which a pair of fixed fins is mounted at a certain configuration whereas the fins have a degree of freedom around their hinge lines in the second group. Selecting the maximum angular deflection of the fins and autopilot switching duration as the comparison criteria, the quantities consisting of the final miss distance from the designated target point and time of flight are calculated for the designated simulation cases according to different engagement scenarios. In the related computer simulations, the linear homing guidance (LHG) law is chosen as the guidance strategy and the effect of the side wind is also taken into consideration.

Figure 1. 81 mm Precision Air-Dropped Guided Mortar (ADM) with Two Fins-General Dynamics [28]

Figure 2. 81 mm Precision Air-Dropped Guided Munition (ADM) with Four Fins-General Dynamics [28]

Figure 3. Guided Projectile Released from an Air Platform in a Vertical Manner [29]

2. GUIDANCE KIT GEOMETRY AND CONTROL APPROACH

The guidance kit which is mounted upon the nose of the unguided mortar projectile is composed of a fuze, rotor outer ring having a pair of control fins, i.e. fins, actuator rotating the rotor outer ring, sensors, electronic cards, and battery as depicted in Figure 4. In this configuration, a brushless alternating current (BLAC) type electrical motor is considered.

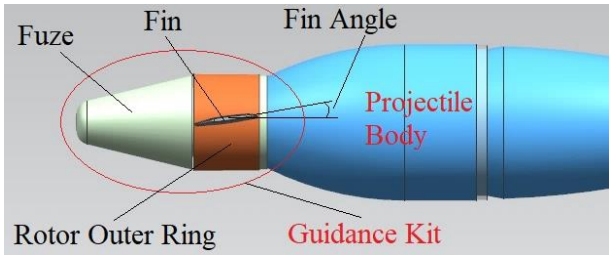

Figure 4. Considered Guidance Kit Geometry

Using the guidance kit introduced above, the motion control of the mortar projectile is planned to be conducted. In the designed scheme, the angular positions of the fins are supplied by the rotation of the rotor outer ring. Namely, once the fin pair is deployed in a horizontal manner, the correponding control of the guided projectile is carried out in its pitch plane. In a similar way, the vertical orientation of the fins indicates the yaw plane control. As implied, the pitch and yaw controls are not performed simultaneously but they follow a sequence each section of which is called switching duration.

In the present study, two different situations are dealt with in the sense of the movement of the fins. In the first case, the fins are taken to be fixed on the rotor outer ring. On the contrary, the second configuration regards the degree of freedom of the fins around their hinge lines. The performance characteristics of both of these configurations are evaluated for a number of projectile-target engagement scenarios.

3. DYNAMIC MODELING OF THE GUIDED PROJECTILE

The equations of motion of the guided mortar projectile under consideration can be ensured with the following way [30]:

$$\dot{u} - rv + qw = (X + X_T)/m + g_x \quad (1)$$
$$\dot{v} + ru - pw = (Y + Y_T)/m + g_y \quad (2)$$
$$\dot{w} - qu + pv = (Z + Z_T)/m + g_z \quad (3)$$
$$\dot{p} = L/I_a \quad (4)$$
$$\dot{q} - pr = (M + M_T)/I_t \quad (5)$$
$$\dot{r} + pq = (N + N_T)/I_t \quad (6)$$

In the expresssions above, the forthcoming definitions are introduced as the variables stand for the longitudinal, lateral, and vertical components of the relevant vectorial quantity in the fixed body reference frame of the projectile (F_b):

m: Mass of the projectile

I_t and I_a: Lateral and axial moment of inertia components

p, q, and r: Components of the angular velocity vector in roll, pitch and yaw directions

u, v, and w: Components of the linear velocity vector

X, Y, and Z: Components of the aerodynamic force vector at the centre of mass of the projectile

L, M, and N: Components of the aerodynamic moment vector at the projectile body

X_T, Y_T, and Z_T: Components of the thrust force vector at the centre of mass of the projectile

L_T, M_T, and N_T: Components of the thrust misalignment moment vector on the projectile body

g_x, g_y, and g_z: Components of the gravity vector at the centre of mass of the projectile

Assuming that the roll component of the angular velocity vector happens to be very low, i.e. p, the expressions (2), (3), (4), (5) and (6) that describe the dynamic behavior of the guided projectile can be simplified to the following equations in the pitch and yaw planes [30]:

$$\dot{w} - qu = (Z/m) + g_z \quad (7)$$
$$\dot{q} = M/I_t \quad (8)$$
$$\dot{v} + ru = (Y/m) + g_y \quad (9)$$
$$\dot{r} = N/I_t \quad (10)$$

The aerodynamic moment and force components Y, Z, M, and N given in equations (7) through (10) can be expressed as follows [30]:

$$Y = C_y q_\infty S_M \quad (11)$$
$$Z = C_z q_\infty S_M \quad (12)$$
$$M = C_m q_\infty S_M d_M \quad (13)$$
$$N = C_n q_\infty S_M d_M \quad (14)$$

Respectively q_∞, S_M, d_M represent the dynamic pressure acting on the projectile, cross-sectional area of the projectile, and projectile diameter. In the above equations, the aerodynamic parameters represented by C_z, C_y, C_n, and C_m can be formulated depending on the side-slip angle (β), angle of attack (α), elevator angle (δ_e), rudder angle (δ_r), q, and r in the next manner [30]:

$$C_y = C_{y_\beta}\beta + C_{y_\delta}\delta_r + C_{y_r}[d_M/(2v_M)]r \quad (15)$$
$$C_z = C_{z_\alpha}\alpha + C_{z_\delta}\delta_e + C_{z_q}[d_M/(2v_M)]q \quad (16)$$
$$C_m = C_{m_\alpha}\alpha + C_{m_\delta}\delta_e + C_{m_q}[d_M/(2v_M)]q \quad (17)$$
$$C_n = C_{n_\beta}\beta + C_{n_\delta}\delta_r + C_{n_r}[d_M/(2v_M)]r \quad (18)$$

Here, as v_M demonstrates the absolute value of vector corresponding to the linear velocity of the projectile, the stability derivatives expressed by C_{y_β}, C_{y_δ}, C_{y_r}, C_{z_α}, C_{z_δ}, C_{z_q}, C_{m_α}, C_{m_δ}, C_{m_q}, C_{n_β}, C_{n_δ} and C_{n_r} depending on the mach number (M_∞) are instantaneously updated during the computer simulations [30].

4. MORTAR PROJECTILE GUIDANCE LAW

The guided mortar projectile is oriented to the intended target point using the LHG law which aims at keeping the projectile on a triangle, namely the collision triangle, designated by the predicted intercept point of the missile and intended target. Denoting the duration from the initial time (t_0) to the end of the intercept (t_F) as Δt, the guidance command for the flight path angle component of the missile in the yaw plane (η_m^c) is determined in the following manner so that $cos(\gamma_m) \neq 0$ [30]:

$$\eta_m^c = arctan\left[\left(v_{Ty}\Delta t - \Delta y\right)/\left(v_{Tx}\Delta t - \Delta x\right)\right] \quad (19)$$

Likewise, the pitch plane form of the guidance command (γ_m^c) can be derived as given below [30]:

$$\gamma_m^c = arctan\left[\frac{\Delta z - v_{Tz}\Delta t}{\left(v_{Tx}\Delta t - \Delta x\right)cos(\eta_m) + \left(v_{Ty}\Delta t - \Delta y\right)sin(\eta_m)}\right] \quad (20)$$

In the expressions above Δ_x, Δ_y, and Δ_z demonstrate components of the relative position vector between the missile and target. Moreover, and v_{Tx}, v_{Ty}, and v_{Tz} stand for the components of the target velocity vector [30].

5. PROJECTILE CONTROL SYSTEM

The projectile control system, i.e. autopilot, designed to convert the guidance commands of the LHG law into physical motion is designed such that it operates in a separate manner in the pitch and yaw planes in a sequential manner. Hence, the closed loop transfer function between the desired and actual flight path angles in both the pitch plane (γ_{md} and γ_m) can be obtained in the following manner [30]:

$$\frac{\gamma_m(s)}{\gamma_{md}(s)} = \frac{n_{\gamma 3}s^3 + n_{\gamma 2}s^2 + n_{\gamma 1}s + 1}{d_{\gamma 4}s^4 + d_{\gamma 3}s^3 + d_{\gamma 2}s^2 + d_{\gamma 1}s + 1} \quad (21)$$

where the parameters $n_{\gamma 1}$, $n_{\gamma 2}$, $n_{\gamma 3}$, $d_{\gamma 1}$, $d_{\gamma 2}$, $d_{\gamma 3}$, and $d_{\gamma 4}$ involve the autopilot gains, projectile diameter, components of the moment of inertia terms of the projectile, components of the velocity vector, q_∞, and aerodynamic gains. From equation (21), the characteristic polynomial happens to be in the forthcoming fashion:

$$D(s) = d_{\gamma 4}s^4 + d_{\gamma 3}s^3 + d_{\gamma 2}s^2 + d_{\gamma 1}s + 1 \quad (22)$$

Thus, the autopilot gains can be obtained by means of the well-known pole placement approach in which the next fourth-order Butterworth polynomial is utilized by regarding the damping ratio (ζ) to be 0.707:

$$B_4(s) = (1/\omega_c^4)s^4 + (2.613/\omega_c^3)s^3 + (3.414/\omega_c^2)s^2 + (2.613/\omega_c)s + 1 \quad (23)$$

where ω_c stands for the desired bandwidth of the autopilot. In a similar case, the transfer function can be adapted from the transfer function attained for the pitch plane by introducing $n_{\eta 1}$, $n_{\eta 2}$, $n_{\eta 3}$, $d_{\eta 1}$, $d_{\eta 2}$, $d_{\eta 3}$, and $d_{\eta 4}$ in the yaw plane [30] :

$$\frac{\eta_m(s)}{\eta_{md}(s)} = \frac{n_{\eta 3}s^3 + n_{\eta 2}s^2 + n_{\eta 1}s + 1}{d_{\eta 4}s^4 + d_{\eta 3}s^3 + d_{\eta 2}s^2 + d_{\eta 1}s + 1} \quad (24)$$

6. ENGAGEMENT MODEL

The following relationships can be written for the distance corresponding to the line-of-sight between the projectile and the intended target (r_T/M) and for the orientation angles to the pitch and yaw planes (λ_p and λ_y) [30]:

$$r_{T/M} = \sqrt{\Delta x^2 + \Delta y^2 + \Delta z^2} \quad (25)$$

$$\lambda_p = arctan\left[-\Delta z\, cos\left(\lambda_y\right)/\Delta x\right] \quad (26)$$

$$\lambda_y = arctan(\Delta y/\Delta x) \quad (27)$$

Assuming that the component of r_T/M in vertical sense occurs almost zero ($\Delta_z=0$) since it is a surface target, the final miss distance from the target at the termination of the engagement (d_{miss}) can be determined by the use of the equation below [30]:

$$d_{miss} = \sqrt{\Delta x^2(t_F) + \Delta y^2(t_F)} \quad (28)$$

where t_F stands for the time value at the end on the engagement.

7. COMPUTER SIMULATIONS

In the present study, a mortar projectile released towards a stationary surface target at a specified altitude (z_{P0}) from an unmanned aerial platform crusing at a constant low speed (v_{P0}) is taken into considerations. As LM and x_{TF} denote the total length of the guided projectile and the longitudinal distance to the target when the projectile is dropped from the platform, respectively, the related simulations are carried out in the computer environment by regarding the data presented in Table 1 [31].

The miss distance from the target and time of flight values of the guided projectile are given in Table 2 and Table 3 according to the angular deflection of the fin and autopilot switching quantities as well as the side wind value for all the 18 specified cases. In Table 2 and Table 3, the fixed and rotating conditions of the fins are also considered. The sample plots belonging to the engagement geometries, projectile speed, nose kit commands, and motor angle are shown in Figure 5 through Figure 13.

Gerilme yığılma faktörü; bir malzemedeki şekilsel sürekliliğin bozulması ile gerilmede ani artışın sebep olduğu katsayı değeridir. Bir parça üzerinde; delik, kanal, oyuk, çıkıntı vb. olduğunda bu şekilsel farklılığın olduğu yerde gerilme değerinde ani artışlar görülür. Bu sebeple, şekilsel sürekliliğin bozulduğu veya şeklin değişime uğradığı yerlerde maksimum gerilme görülür. Mühendislik olarak bu değer (Denklem 1) biçiminde ifade edilir. Malzeme hangi tür gerilme/gerilmelere maruz kalmış ise toplam gerilme cinsinden σ_{normal} değeri hesap edilir. $\sigma_{emniyet}$ değeri ise o malzemenin emniyetli dayanım değeridir.

$$K_t = \frac{\sigma_{emniyet}}{\sigma_{normal}} \quad (1)$$

Table 1. Parameter values in the computer simulations

Parameter	Numerical Value	Parameter	Numerical Value
d_M	50 mm	vP0	0.8·Mach (=272 m/s)
L_M	500 mm	zp0	1000 m
m	15 kg	xTF	1000 m
I_a	0.018 kg·m2	ωc	10 Hz
I_t	5.005 kg·m2	ζ	0.707

Table 2. Results of the the computer simulations without side wind

Case Number	Fin Angle	Autopilot Switching (s)	Miss Distance (m)		Time of Flight (s)	
			Fixed Fin	Rotating Fin	Fixed Fin	Rotating Fin
1	1°	0.2	95.700	1.355	5.115	5.200
2		0.5	79.039	95.495	5.067	4.674
3		1.0	68.876	207.707	5.088	4.250
4	5°	0.2	459.227	1.355	6.997	5.200
5		0.5	333.240	95.495	7.190	4.674
6		1.0	356.974	207.707	7.229	4.250
7	10°	0.2	368.985	1.355	5.296	5.200
8		0.5	73.998	95.495	9.725	4.674
9		1.0	147.076	207.707	8.568	4.250

Table 3. Data acquired from the computer simulations with the side wind speed of 5 m/s

Case Number	Fin Angle	Autopilot Switching (s)	Miss Distance (m)		Time of Flight (s)	
			Fixed Fin	Rotating Fin	Fixed Fin	Rotating Fin
10	1°	0.2	107.738	34.957	5.200	5.381
11		0.5	104.029	147.921	5.068	5.057
12		1.0	92.714	299.335	5.088	4.047
13	5°	0.2	476.736	34.957	7.352	5.381
14		0.5	364.585	147.921	7.032	5.057
15		1.0	376.091	299.335	7.785	4.047
16	10°	0.2	524.728	34.957	4.661	5.381
17		0.5	313.032	147.921	4.950	5.057
18		1.0	164.509	299.335	7.962	4.047

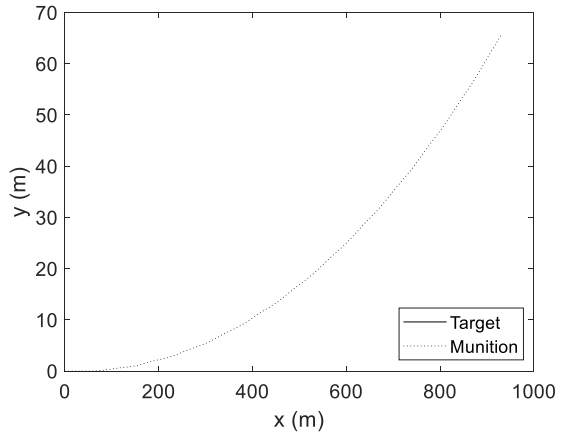

Figure 5. Engagement geometry on the horizontal plane for the projectile and target for case 1 at fixed fin condition

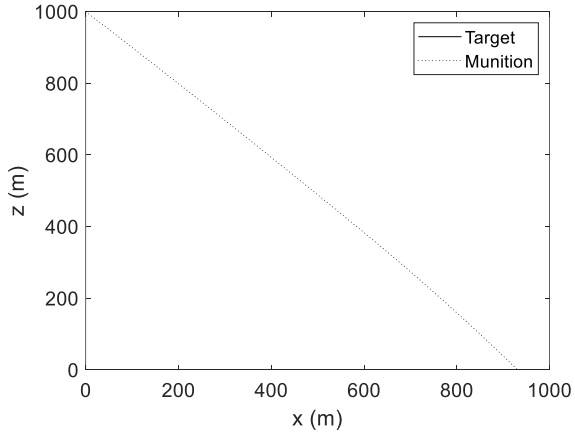

Figure 6. Engagement geometry on the vertical plane for the projectile and target for case 1 at fixed fin condition

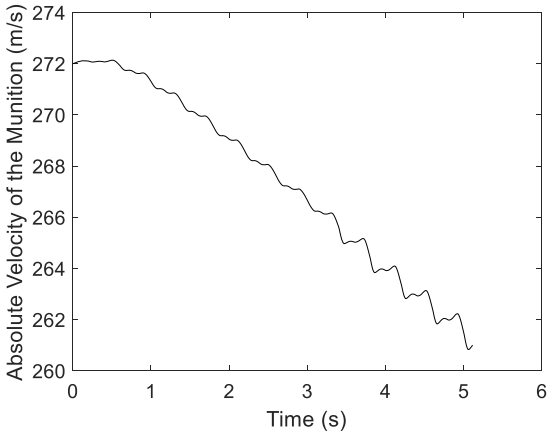

Figure 7. Time change of the projectile speed for case 1 at fixed fin condition

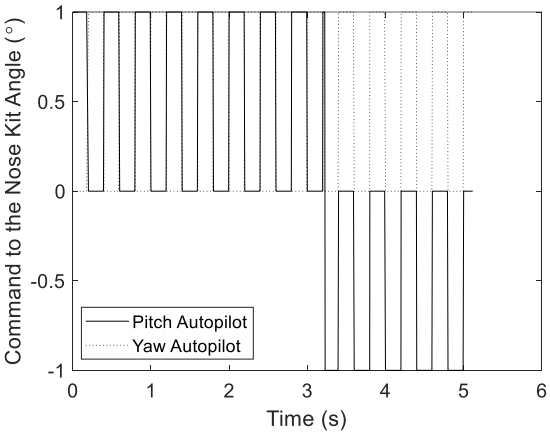

Figure 8. Time change of the command to the nose kit angle for case 1 at fixed fin condition

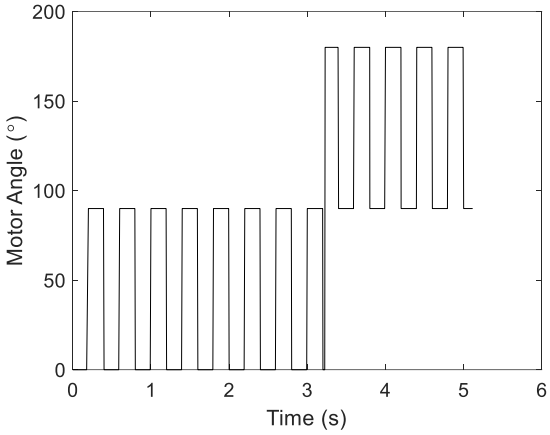

Figure 9. Time change of the motor angle for case 1 at fixed fin condition

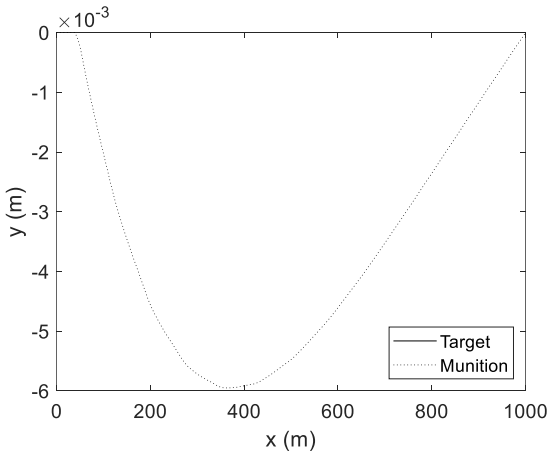

Figure 10. Engagement geometry on the horizontal plane for the projectile and target for case 1 at rotating fin condition

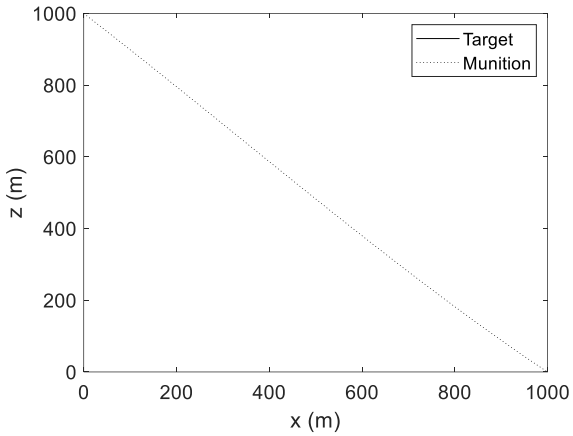

Figure 11. Engagement geometry on the vertical plane for the projectile and target for case 1 at rotating fin condition

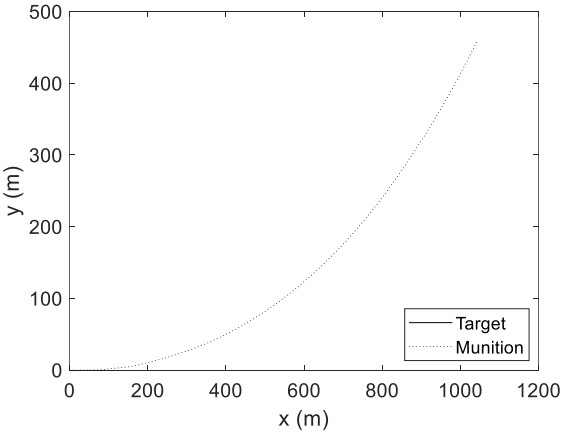

Figure 12. Engagement geometry on the horizontal plane for the projectile and target for case 4 at fixed fin condition

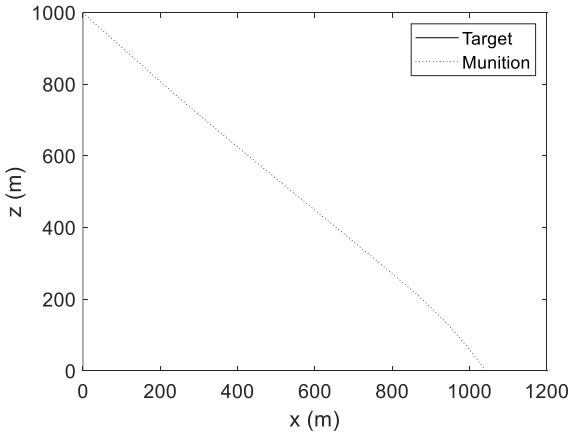

Figure 13. Engagement geometry on the vertical plane for the projectile and target for case 4 at fixed fin condition

5. DISCUSSION AND CONCLUSION

The simulation data submitted in Table 2 and Table 3 indicate that the rotating find leads smaller miss distance for the shortest autopilot switching duration considered for both windless and windy cases. Once the switching duration increases, the smaller miss distance is attained with the fixed fins. An interesting point shown from the acquired data belonging to the cases with the rotating fins is that the final miss distance quantities do not change for the same switching duration when the fin angle becomes different. However, the guided projectile with the fixed fins has a growing pattern as the fin angle gets larger. Also, although the results are obtained for the initial speed of 0.8 Mach in the present study, the proposed method is applicable up to the projectile speed of 0.2 Mach for the unmanned aerial platforms.

- Comparing these two configurations in the sense of the time of flight, it can be stated that the configuration with the rotating fins yields smaller durations except cases 1 and 10.
- As expected, the results reveal that both the miss distance and time of flight become larger when the wind acts on the projectile.
- Consequently, the guided projectile geometries with rotating fins on a rotary rind result in small final miss distance and time of flight quantities in general.

DECLARATION OF ETHICAL STANDARDS

The author(s) of this article declare that the materials and methods used in this study do not require ethical committee permission and/or legal-special permission.

AUTHORS' CONTRIBUTIONS

Bülent ÖZKAN: Put forward the first idea on the stated, developed and wrote the manuscript, contributed at all stages of the article.

Harun GÖKÇE: Performed the numeric examples and tables. Also, analyzed some calculations and results.

CONFLICT OF INTEREST

There is no conflict of interest in this study.

REFERENCES

[1] Özkan B. and Gökçe, H. "Guidance and control of a surface-to-surface projectile using a nose actuation kit", ***European Journal of Science and Technology***, 22, 282-292 (2021).

[2] Çantaş, Y. and Akbulut, A. "Design and simulation of autopilot for fixed wing aircraft", ***Politeknik Dergisi***, 25, 4, 1523-1534 (2022).

[3] Gürgöze, G. and Türkoğlu, İ. "Development of experimental setup for determining the parameters of DC motors used in mobile robots", ***Politeknik Dergisi***, 25, 1, 115-121, (2022).

[4] Yüksek, G., Mete, A. N., and Alkaya, A. "LQR and GA based PID parameter optimization: liquid level control application", ***Politeknik Dergisi***, 23, 4, 1111-1119 (2020).

[5] Baranowski, L. "Equations of motion of a spin-stabilized projectile for flight stability testing" ***Journal of Theoretical and Applied Mechanics***, 51, 1, 235-246, (2013).

[6] Fresconi, F., Celmins, I., Silton, S., and Costello, M.. "High maneuverability projectile flight using low cost components", ***Aerospace Science and Technology***, 41, 175-188, (2015).

[7] Yin, J., Wu, X., Lei, J., Lu, T., and Liu, X. "Canard interference on the Magnus effect of a fin-stabilized spinning missile", ***Advances in Mechanical Engineering***, 10, 7, 1-16 (2018).

[8] Fresconi, F., Cooper, G., Celmins, I., DeSpirito, J., and Costello, M. "Flight mechanics of a novel guided spin-stabilized projectile concept", ***Proc. ImechE, Part G: Journal of Aerospace Engineering***, 226, 327-340 (2011).

[9] Ilg, M. D. "Guidance, navigation, and control for munitions" Thesis, ***Drexel University***, (2008).

[10] Fresconi, F. and Plostins, P. "Control mechanism strategies for spin-stabilized projectiles", ***Army Research Laboratory Report***, USA, (2008).

[11] Eroğlu, M. "Design and Control of Nose Actuation Kit for Position Correction of Spin Stabilized Munitions under Wind Effect" Thesis, ***Middle East Technical University***, Ankara, Turkey, (2016).

[12] Habash, Y. "Roll controlled guided mortar", ***NDIA Joint Armaments Conference***, Seattle, WA, (2012).

[13] Fresconi, F. and I. Celmins. "Experimental flight characterization of spin-stabilized projectiles at high angle of attack", ***Army Research Laboratory Report***, USA, (2017).

[14] Rogers, J. and Costello, M. "Design of a roll-stabilized mortar projectile with reciprocating canards", ***Journal of Guidance Control Dynamics***, 33, 4, 1026-1034, (2010).

[15] Qing, Y. and Chunsheng, L. "A differential game-based guidance law for an accelerating exoatmospheric missile", ***Asian Journal of Control***, 19, 3, 1205-1216, (2017).

[16] Guo, J., Liu, L., and Sun, Y. "Design of attitude control system for guided projectile", ***3rd International Conference on Applied Machine Learning***, Changsha, 482-486, (2021).

[17] Habash, Y. "Roll control guided mortar, NDIA Joint Armaments Conference", ***Seattle Washington, USA***, (2012).

[18] Shen, Y., Yu, J., Luo, G., Ai, X., Jia, Z., Chen, F. "Observer-based adaptive sliding mode backstepping output-feedback DSC for spin-stabilized canard-controlled projectiles", ***Chinese Journal of Aeronautics***, 30, 3, 1115-1126, (2017).

[19] Chen, Q., Wang, X., Yang, J., and Wang, Z. "Acceleration tracking control for a spinning glide guided projectile with multiple disturbances", ***Chinese Journal of Aeronautics***, 33, 12, 3405-3422, (2020).

[20] http://pena-abad.blogspot.com/2010/04/ air-dropped-mortar-successfully.html, Erişim: 21 May 2021.

[21] Jiwei, G. and Yuan-Li Cai, C. "Three-dimensional impact angle constrained guidance laws with fixed-time convergence", ***Asian Journal of Control***, 19, 6, 2240-2254, (2017).

[22] Gkritzapis, D. N., Margaris, D. P., Panagiotopoulos, E. E., Kaimakamis, G., and Siassiakos, K. "Prediction of the impact point for a spin and fin-stabilized projectiles", ***WSEAS Transactions on Information Science and Applications***, 5, 12, 1667-1676, (2008).

[23] Cooper, G. R. and Costello, M. "Trajectory prediction of spin-stabilized projectiles with a liquid payload", ***Journal of Spacecraft and Rockets***, 48, 4, 664-670, (2011).

[24] Şahin, K. D. "A pursuit evasion game between an aircraft and a missile", MSc Thesis, ***Middle East Technical University***, Ankara, Turkey, (2002).

[25] Zhang, X., Yao, X., and Zheng, Q. "Impact point prediction guidance based on iterative process for dual-spin projectile with fixed canards", ***Chinese Journal of Aeronautics***, 32, 8, 1967-1981, (2019).

[26] Fresconi, F. "Guidance and control of a projectile with reduced sensor and actuator requirements", ***Journal of Guidance Control and Dynamics***, 34, 6, 2011.

[27] Jiang, S., Tian, F., Sun, S., and Liang, W. "Integrated guidance and control of guided projectile with multiple constraints based on fuzzy adaptive and dynamic surface", ***Defence Technology***, 16, 1130-1141, (2020).

[28] https://www.gd-ots.com/wp-content/uploads/2017/11/ 81mm-Air-Dropped-Guided-Mortar-ADM.pdf, Date of Access: 21.05.2021.

[29] https://www.joongang.co.kr/article/23447397#home, Date of Access: 14.02.2023.

[30] Özkan, B., Özgören, M. K., Mahmutyazıcıoğlu, G. "Performance comparison of the notable acceleration-and angle-based guidance laws for a short-range air-to-surface missile", ***Turkish Journal of Electrical Engineering and Computer Sciences***, 25, 3591-3606, (2017).

[31] Milinović, M., Jerković, D., Jeremić, O., and Kovač, M. "Experimental and simulation testing of flight spin stability for small calibre cannon projectile", ***Journal of Mechanical Engineering***, 58, 6, 394-402, (2012).